Shaping the surface of Borofloat 33 glass with ultrashort laser pulses and a spatial light modulator

Krystian L. Wlodarczyk* and Duncan P. Hand

Institute of Photonics and Quantum Sciences, School of Engineering and Physical Sciences, Heriot-Watt University, Edinburgh EH14 4AS, UK

*Corresponding author: K.L.Wlodarczyk@hw.ac.uk

Received 16 October 2013; revised 4 February 2014; accepted 7 February 2014; posted 10 February 2014 (Doc. ID 199309); published 13 March 2014

We demonstrate an application of a liquid-crystal-based spatial light modulator (LC-SLM) for the parallel generation of optically smooth structured surfaces on Borofloat 33 glass. In this work, the picosecond laser beam intensity profile of wavelength 515 nm is spatially altered by a LC-SLM, and then delivered to the workpiece in order to generate surface deformations whose shape corresponds to the image generated by the LC display. To ensure that localized melting occurs without ablation, the glass surface is covered by a thin layer of graphite prior to laser treatment to provide increased linear absorption of the laser light. After laser treatment the residual graphite layer is removed using methanol and the whole sample is annealed for 1 h at a temperature of 560 °C, making the laser-induced surface deformations optically smooth. © 2014 Optical Society of America

OCIS codes: (140.3390) Laser materials processing; (160.2750) Glass and other amorphous materials; (230.6120) Spatial light modulators; (220.4000) Microstructure fabrication; (320.7090) Ultrafast lasers.

http://dx.doi.org/10.1364/AO.53.001759

1. Introduction

When a solid material is processed by high-intensity laser pulses of duration of less than a nanosecond, the laser-machined area is very often characterized by low surface quality. This is because such short laser pulses remove material with little melting, creating a surface containing microscale roughness that significantly scatters the incident light. To overcome this problem and provide optically smooth surfaces, it is better to use laser machining conditions that provide melting in addition to ablation. One example of such an approach is the YAGboss process [1] in which nanosecond laser pulses of wavelength 355 nm are focused using a cylindrical lens onto a metal workpiece (Chromflex stainless steel) in order to melt its surface and generate depressions with a well-controlled depth via a localized melt flow process. In this approach, the melt flow is driven by the laser-induced gradient of surface tension. By synchronizing laser pulses with precise movement of the workpiece, the YAGboss process has been used to generate sinusoidal gratings with a spatial period of 8 μm, suitable for applications as scales in high-precision optical positioning encoders [1].

Even though the YAGboss process has been established for metals, currently it cannot be used for optical (silicon-oxide-based) glasses because UV nanosecond laser pulses are unable to controllably generate a molten layer at the glass surface due to the low linear absorption of these materials in the range of wavelengths between 300 nm and 3.5 μm. However, the relatively high absorption and low reflectivity of optical glasses at 10.6 μm means that a CO_2 laser can be used for shaping (melting) the

1559-128X/14/091759-07$15.00/0

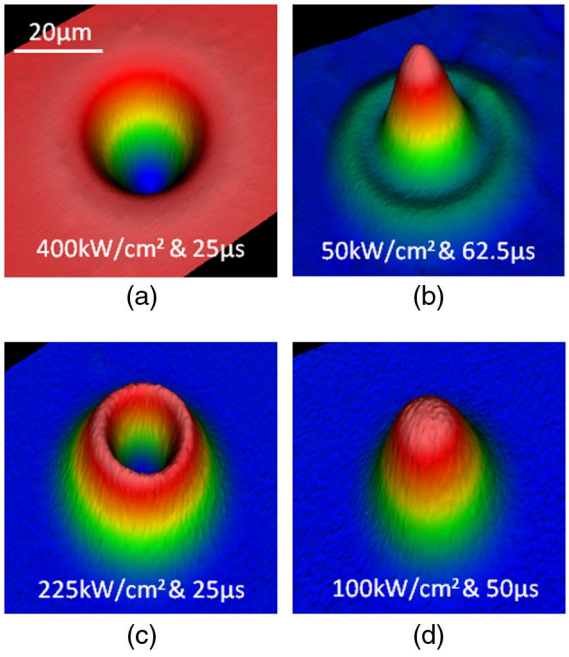

Fig. 1. Surface deformations produced by a single CO_2 laser pulse: (a) crater in fused silica (HPFS 7980, Corning), (b) sombrero-shaped bump in lead-silicate glass (SF57, Schott AG), (c) ring, and (d) dome-shaped bump in borosilicate glass (Borofloat 33, Schott AG). The peak irradiance and pulse duration values used for generating the features are shown in the figure.

surface of these brittle materials. Although many features, such as craters, rings, dome-shaped bumps, and sombrero-shaped bumps, can be produced by using CO_2 laser pulses, as shown in Fig. 1 [2], the long laser wavelength means that the laser spot size is limited to tens of micrometers, and hence it is very difficult to generate surface features smaller than 20–30 μm in diameter.

In this paper, we investigate the interaction of borosilicate glass (Borofloat 33, Schott AG) with nanosecond and picosecond laser pulses in order to find conditions for melting the glass surface at wavelengths ($\lambda = 343$, 515, 532, 1030, and 1064 nm) at which this material is normally transparent. The aim of this work was to produce optically smooth structured surfaces, e.g., sinusoidal gratings with a spatial period of less than 30 μm. In this work, we also study the interaction of such laser beams with "opaque" Borofloat 33 glass, i.e., when its surface is covered by a thin layer of graphite prior to laser treatment in order to increase the linear absorption of the laser light. Finally, this paper reports the use of a liquid-crystal-based spatial light modulator (LC-SLM) for parallel shaping the glass surface, demonstrating a promising approach for the flexible generation of optically smooth structures on glass.

As reported elsewhere [3–8], a LC-SLM can be used to split the output laser beam in an array of beamlets in order to machine a workpiece simultaneously with many laser beams, thereby increasing significantly the processing throughput. This approach has been successfully used to inscribe "simple" patterns on the glass surface by Hayasaki *et al.* [3]. In our work, however, we use a LC-SLM for the generation of more complex patterns than regularly arranged dots or microgrooves, and instead of ablating the glass we control the pulse energy to only melt the workpiece surface so that the laser-machined area remains optically smooth.

We chose Borofloat 33 glass as a test workpiece for two reasons. The first is that this glass is characterized by a relatively low coefficient of thermal expansion (CTE = 3.3 ppm/K), and so there is a low risk of material cracking when cooled rapidly between sequential laser pulses and after laser treatment [9]. The second reason is that this material reveals a tendency to "bump" when sufficient local heat is generated, for example, by a CO_2 laser beam, as shown in Figs. 1(c) and 1(d). Although optical glasses with a very low CTE (<3.3 ppm/K) can be effectively machined with a CO_2 laser [9–12], the surface of these glasses is less vulnerable to thermally induced deformations. For instance, CO_2 laser-induced deformations in fused silica are in the form of shallow depressions with a masked sombrero-shaped base [10–12]. The depth of the depressions is typically less than 200 nm, whereas the peak-to-valley height of the sombrero-shaped base is only in the range of tens of nanometers (for a single laser beam pass). As explained in [10–12], the depressions result from a local densification of the glass, whereas the sombrero-shaped base is a result of the laser-induced gradient of surface tension (the Marangoni effect).

In general, Borofloat 33 is a clear and transparent glass that is used in optics, optoelectronics, photovoltaics, and biotechnology. Due to its outstanding thermal properties, such as a low CTE, high thermal shock resistance, and the ability to withstand temperatures up to 450°C for long periods, this glass is also used in home appliances (e.g., interior oven doors), the chemical industry (e.g., reaction vessels), and lighting (e.g., protective panels for spotlights).

2. Nanosecond Laser Processing of Borofloat 33

A diode-pumped, *Q*-switched Yb:YVO_4 laser (Spectra Physics Lasers Inc.) was used to study the interaction of Borofloat 33 glass with nanosecond laser pulses at wavelengths (λ) of 532 and 1064 nm. This laser provides pulses of approximately 65 ns duration with average powers of up 20 and 35 W at $\lambda =$ 532 and 1064 nm, respectively, with a variable pulse repetition frequency (PRF) in the range of 15–100 kHz. The laser beam was delivered to the workpiece via a galvo-scanner equipped with a flat field (F-theta) lens, giving an approximately 30 μm diameter spot at the focal plane.

We attempted to identify laser parameters that would provide controllable melting of as-manufactured Borofloat 33 glass. Different values of the laser power were tested ($P = 0.5$–10 W) for a range of different scan speeds ($v = 1$, 2, 5, 10, and 20 mm/*s*), PRFs (PRF = 15 and 100 kHz), and wavelengths ($\lambda = 532$ and 1064 nm). In all of these cases, however,

there was insufficient absorption to melt or even gently ablate the glass surface without material cracking. Microcracks started to appear at an average laser fluence of approximately 28 J/cm^2 (i.e., $P = 3$ W at 15 kHz).

In order to enhance the linear absorption of the laser light, a thin layer of graphite from an aerosol can (Graphit33, Kontakt Chemie) was manually sprayed onto the glass surface prior to laser treatment. The graphite layer was reasonably uniform, and its thickness was in the range of 20–30 μm, depending on the sample used. Using this simple approach, we achieved "*opaque*" glass. In this case it was possible to machine glass with a laser fluence of 5 J/cm^2 ($P = 0.5$ W at 15 kHz). The focused laser beam was moved across the workpiece surface in order to generate shallow grooves on the glass surface. After laser treatment, the surface was cleaned with methanol and annealed at a temperature of 560°C for 1 h in order to release the laser-induced stresses in the glass.

Figure 2 shows 25 μm wide grooves, which were produced by the focused beam, using nanosecond laser pulses at $\lambda = 1064$ nm, $f = 15$ kHz, $P = 3$ W, and $v = 10$ mm/s. The separation distance between laser scans was chosen to be 50 μm. At these laser machining conditions, the grooves were very shallow with the peak-to-valley value of approximately 40 nm. The 3D profile and cross section of the structure was obtained with the Zygo noncontact measurement profiler. Small lobes around the grooves suggest that either resolidification or local melting of the glass (and graphite) occurred during the laser process. A similar effect was observed in graphite-coated metals by Carey *et al.* [13].

By applying a shorter (25 μm) separation distance between laser scans and reducing the laser power and scanning speed, it was possible to produce sinusoidal gratings with a range of different amplitudes (peak-to-valley values). An example of such a grating is shown in Fig. 3. This structure was generated using the laser power of 0.5 W and a scan speed of 1 mm/s, giving a peak-to-valley of approximately 165 nm. The rms value along the laser-scanned tracks was measured to be less than 25 nm. Figure 3 also shows a high-contrast optical image of the grating, revealing that some residual graphite is present at the glass surface, even though the glass was cleaned with methanol and kept in a furnace at a temperature of 560°C for 1 h. We assume that the graphite was firmly bonded to the glass surface during laser treatment, and therefore it cannot be easily

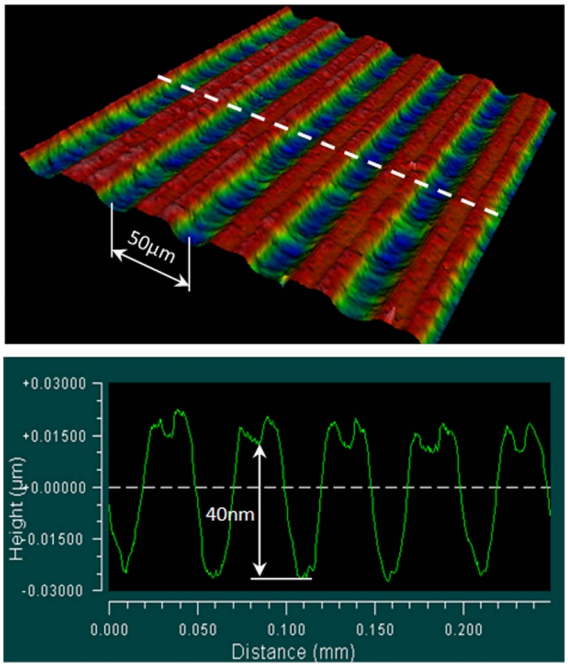

Fig. 2. Grooves produced at the graphite-coated surface of Borofloat 33 glass using nanosecond laser pulses at $P = 3$ W and $v = 10$ mm/s. The profile was taken when the residual graphite was removed and the sample was annealed at 560°C for 1 h.

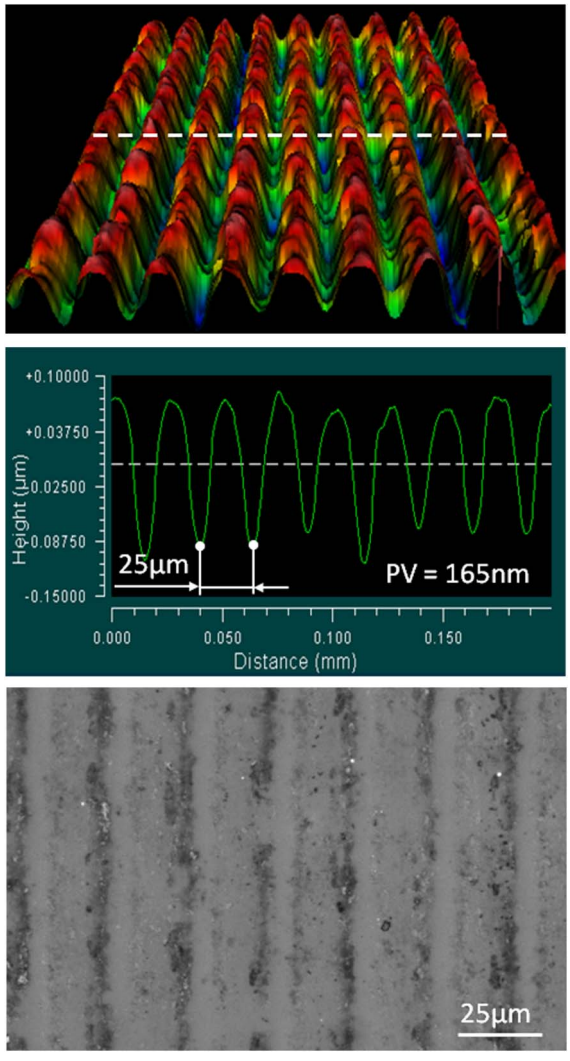

Fig. 3. 3D surface profile, cross section (taken along the dashed line), and optical image of a sinusoidal grating produced in graphite-coated Borofloat 33 glass using nanosecond laser pulses. Laser machining conditions were $P = 0.5$ W, $v = 1$ mm/s, and $\Delta x = 25$ μm.

removed using any alcohol solvent and the annealing process. The grating structure was able to produce a diffraction pattern (in the form of linearly arranged spots) when illuminated by the light from a laser pointer.

3. Picosecond Laser Treatment of Borofloat 33

To study the interaction of Borofloat 33 glass with picosecond laser pulses, we used a thin-disk TruMicro 5250-3C laser (Trumpf) that provided 6 ps laser pulses at a maximum pulse repetition rate of 400 kHz, and three different wavelengths: 343, 515, and 1030 nm. The laser beam was delivered to the workpiece via a high-speed galvo-scanner and an F-theta lens, giving a focused spot diameter (measured at its $1/e^2$ intensity) in the range of 10–35 μm, dependent on the laser wavelength.

No melting effect was observed at the surface of Borofloat 33 glass when machined with picosecond laser pulses, independently of the laser wavelength used. However, craters and fractures were observed. The surface damage threshold of this glass, when machined with a laser beam overlap more than 20% (five pulses per laser spot), was found to be approximately 0.4 J/cm^2 at 343 nm, 1.7 J/cm^2 at 515 nm, and 3.4 J/cm^2 at 1030 nm [14].

In the case of the graphite-coated glass, it was possible to generate very low ridges with an aspect ratio (height to width) of less than 1/250 when the laser operated at $\lambda = 515$ nm and PRF = 400 kHz. The ridges were observed in the "*cleaned*" samples, i.e., in which the residual graphite layer was washed off by methanol. Figure 4(a) shows an example of the ridges generated by a 30 μm diameter laser spot that was moved along the line track with a 2 mm/s speed at $P = 150$ mW. Although each ridge was generated by a different number (N) of laser beam passes, there is no significant height difference between them.

In general, the ridges were found to be produced by local melting of the glass surface. Two mechanisms are involved in the formation of these surface features. The first is the Marangoni effect, in which flow of the melt is driven by the gradient of surface tension that creates either depressions or protrusions, depending on whether the gradient is negative or positive [15]. In our case, the gradient of surface tension was positive, pulling the melt toward the center of the laser-irradiated area (i.e., the hottest site). As reported by others [16,17], the positive gradient of surface tension in Borofloat 33 results from the tendency of the main constituents of this glass, i.e., SiO_2 and B_2O_3, to dissociate at elevated temperatures. The second mechanism is the so-called fictive temperature effect, which can locally alter the density, and hence the volume of glass. The fictive temperature is a term proposed by Tool [18], who suggested that glass that is cooled through the transformation range (the range in which glass becomes a solid) has an identical frozen-in structure to that of its melt at some equilibrium temperature. This means that depending on the cooling rate of glass in the transformation range, the glass network undergoes either faster or slower structural changes, and thus the value of fictive temperature is modified. In general,

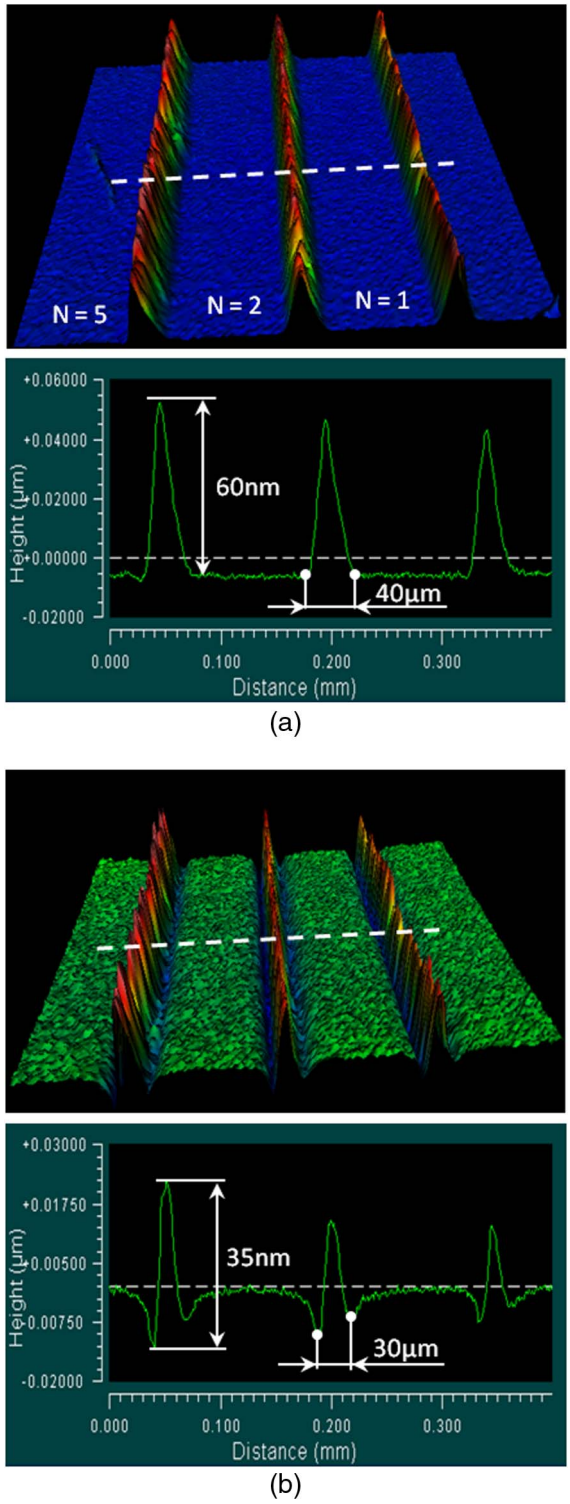

Fig. 4. Ridges generated by a 30 μm diameter laser spot moved along the line track with a speed of 2 mm/s, using PRF = 400 kHz, $P = 150$ mW, and $\lambda = 515$ nm: (a) before and (b) after annealing for 1 h at 560°C. The residual graphite layer was removed before measurement. N value stands for a number of laser passes.

glass cooled rapidly has a higher fictive temperature that the same glass cooled more slowly.

Commercial glasses have a fictive temperature between the strain point and the annealing point because they are cooled slowly in the manufacturing process. However, the value of fictive temperature can be increased (even up to the softening point) if glass is reheated above the annealing point and then is rapidly cooled down. Since glass in our experiment was cooled with a very high cooling rate (possibly more than 10^4 K/s) during laser treatment, this material surely gained a high value of the fictive temperature within the laser-irradiated area, and hence some physical properties of this glass (e.g., refractive index, density) were modified in this region. As reported by Bennett *et al.* [19], an increase of fictive temperature in many silicate glasses results in a decrease of the glass density. This means that the glass volume increases and deformations in the form of bumps or ridges are produced at the glass surface, as observed in our experiments.

The evidence that the laser-induced deformations in Borofloat 33 glass result from an increase of fictive temperature is provided in Fig. 4. This figure shows the cross section of the ridges that was taken (a) immediately after laser treatment and cleaning, and (b) after annealing the glass sample for 1 h at 560°C. Ridges that are shown in Fig. 4(a) are approximately 60 nm high, and their shape results from both the Marangoni effect and a local increase of the fictive temperature within the laser-irradiated area. When the sample was annealed at a temperature of 560°C for 1 h, using a low cooling rate of 2°C per minute, the height of the ridges was reduced, as shown in Fig. 4(b), resulting in no overall change in the glass volume compared with the original sample. This is because the annealing process restored the low value of the fictive temperature, which had been originally gained during the manufacturing process of this glass. The remaining deformations are therefore those generated only by the Marangoni effect, i.e., the flow of the melt within the laser-irradiated area.

4. Parallel Shaping the Surface of Borofloat 33 with SLM

The strong interaction of picosecond laser pulses with Borofloat 33 glass at the wavelength of 515 nm, as presented in the previous section, encouraged us to test a LC-SLM for parallel shaping the glass surface. Figure 5 shows our experimental setup, in which the picosecond laser pulses were delivered to the LC-SLM display (Holoeye LC-R 2500) via a rotatable half-wave plate ($\lambda/2$) in order to obtain the most efficient operation of the optical modulator. The LC-SLM display had a resolution of 1024 × 768 pixels with a pixel size of 19 × 19 μm, and provided an image frame rate of 75 Hz. In this optical arrangement, the LC-SLM operates as a programmable diffractive optical element. The diffractive image produced by the LC-SLM was delivered

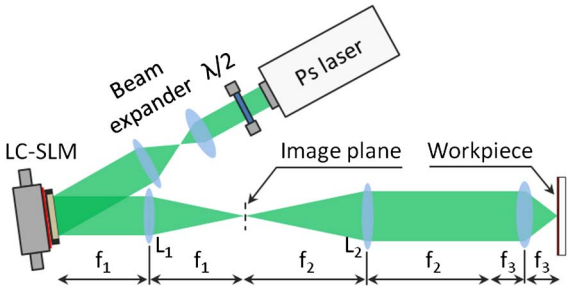

Fig. 5. Experimental setup used for parallel shaping the glass surface with the LC-SLM.

to the workpiece using a 6-f optical system. Since approximately 50% of the incident laser power was undiffracted by the modulator, causing unwanted damage to the glass surface, the undiffracted beam was physically blocked at the first image plane (between L_1 and L_2) using a thin silver wire with an approximately 500 μm bead at its end. The computer-generated holograms (CGHs), which were displayed on the LC-SLM display, were produced using the iterative Fourier transform algorithm (IFTA) [20].

Figure 6 shows the structure of four bumps with square-shaped bases that were produced simultaneously by a 13.33 ms train of picosecond laser pulses (this corresponds to one image frame of the SLM display), using a 400 kHz PRF and an average output laser power of 3.4 W. Each of the four bumps was generated by a 30 × 30 array of beamlets. The profile of the bumps, which are shown in Fig. 6, was taken

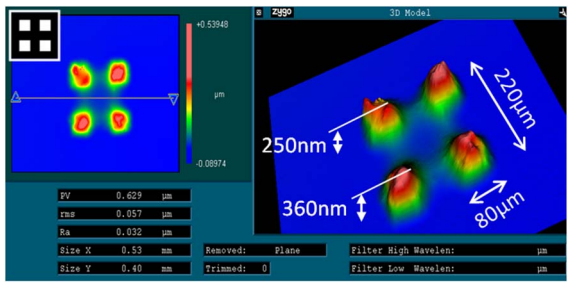

(a)

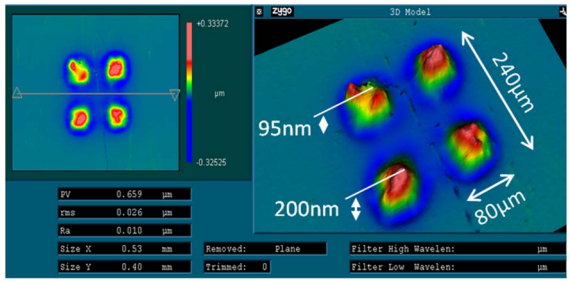

(b)

Fig. 6. Four bumps with square-shaped bases that were generated simultaneously by LC-SLM, which was illuminated by a single 13.33 ms train of 6 ps laser pulses at PRF = 400 kHz and $P = 3.4$ W. The surface profile of the bumps was taken (a) before and (b) after annealing the glass at $T = 560$°C.

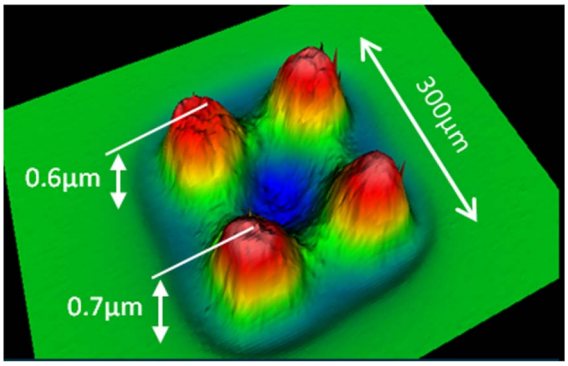

(a)

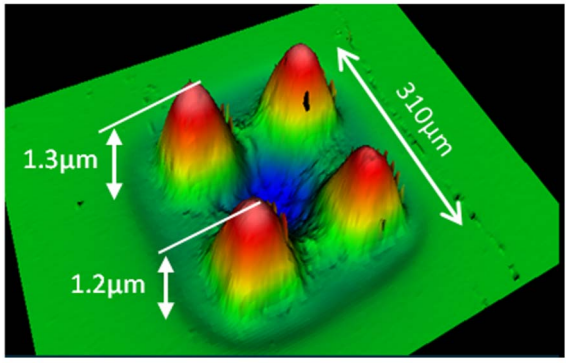

(b)

Fig. 7. Impact of the laser exposure time on the size of the SLM-generated bumps. An average laser power used was 6.5 W, whereas the laser exposure time was (a) 13.33 ms and (b) 213.28 ms (i.e., 16 × 13.33 ms).

(a) before and (b) after annealing the glass for 1 h at a temperature of 560°C. Before the measurement, the glass sample was cleaned with methanol in order to remove the residual graphite layer from its surface. The height of the bumps was measured to be between 250 and 360 nm before annealing and between 95 and 200 nm after annealing. The difference in height between the bumps probably results from the non-uniform intensity distribution of the laser beam across the laser-irradiated area. At this point, it has to be noted that we did not try to optimize the CGH in order to obtain a more uniform intensity distribution within the diffractive image. However, this can be done by (a) designing a CGH for the actual shape of the laser beam delivered to the SLM display, (b) using a feedback closed-loop control for optimizing the CGH [21,22], or (c) using different algorithms for generating a CGH [23,24]. Although the CGH was not ideal, the shape of the bumps was found to be consistent with the target image design, which is shown in the top-left corner of Fig. 6(a).

The height of the bumps can be increased by using either a higher average laser power or a longer laser exposure time, as shown in Fig. 7. In the case of multiple laser exposure, the bumps increase their height due to the longer interaction time of the laser beam with graphite-coated glass, thereby allowing a thin glass layer to stay longer in the molten state.

Energy-dispersive x-ray (EDX) analysis revealed that some amount of carbon (approximately 12% of the atomic percentage) is still present at the glass surface within the laser-irradiated area after the laser treatment and sample cleaning with alcohol. The EDX analysis also showed that the carbon content in Borofloat 33 is reduced (to only a few percent) when glass is annealed for 1 h at 560°C. Based on this result, it can be assumed that the residual graphite migrates deeper into the glass during the annealing process, thereby making the glass surface more optically transparent. Since the melting point of graphite is approximately 3650°C, the graphite definitely cannot be removed from glass at the annealing temperature of 560°C. Nevertheless, the optically smooth surface of the laser-generated structure means that such a structure can potentially be used as an optical component (e.g., a microlens array).

Finally, an example of a sinusoidal structure generated by picosecond laser pulses and the LC-SLM is shown in Fig. 8. This structure was produced at $P = 6.5$ W, using a 4×13.33 ms laser exposure. Although the spatial period of this sinusoid is quite large ($\Lambda = 60$ μm), this is another example of the

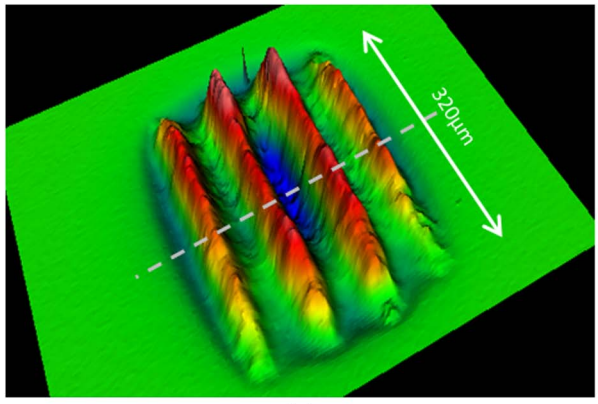

(a)

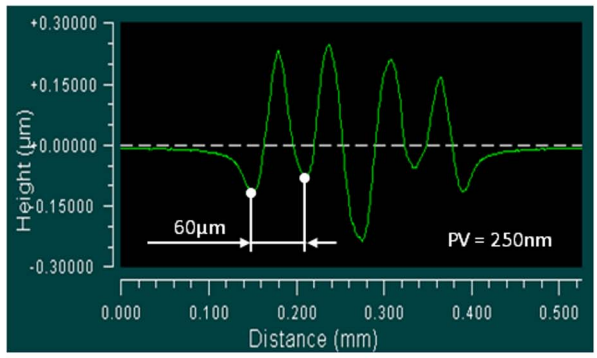

(b)

Fig. 8. Sinusoidal structure produced at the surface of Borofloat 33 glass by LC-SLM, using a 4×13.33 ms laser exposure time and 6.5 W average output laser power: (a) 3D surface profile and (b) cross section of the sinusoidal structure taken along the dashed line shown in (a).

application of a LC-SLM for shaping the glass surface. By synchronizing laser pulses with precise and linear movement of the workpiece, as with the YAGboss process [1], it would be possible to generate very long sinusoidal gratings with an arbitrary spatial period. Such structures can be used, for instance, as scales in optical positioning encoders or U-shaped grooves in micro-optical devices.

5. Conclusions

In this paper we demonstrated techniques for the generation of bespoke optical surfaces using nanosecond and picosecond lasers. By applying graphite onto the glass surface to increase linear absorption, it was possible to generate melt-only processes (with a picosecond laser) or "ablation plus melt" processes (with a nanosecond laser). Although CO_2 lasers remain the most efficient laser sources for shaping the glass surface, they cannot readily produce structures with feature sizes of less than 30 μm. This paper also showed that the use of a LC-SLM opens the opportunity for the generation of structures with an arbitrary shape on glass. We believe that this technique can be used for texturing glass when more complex features (e.g., elliptical, squared, striped bumps) are required. Although a LC-SLM can be easily used for the generation of complex patterns, as demonstrated in our earlier works [25,26], it would be useful to create a theoretical model to simulate the flow of molten glass when driven by an array of laser beams. Such a model may provide more information about the complexity of structures that can be achievable with a LC-SLM.

The research described in this paper was funded by the Engineering and Physical Sciences Research Council (EPSRC), Heriot-Watt Innovative Manufacturing Research Centre (HW-IMRC), grant No. EP/F02553X/1, and our industrial partner Renishaw Plc. (UK). The authors thank Mr. Mark Leonard for helping in the surface profile measurement of samples, and Mr. Jim Buckman for performing the EDX analysis.

References

1. N. J. Weston, D. P. Hand, S. Giet, and M. Ardron, "A method of forming an optical device," patent WO/2012/038707 (29 March 2012).
2. K. L. Wlodarczyk, "Surface deformation mechanisms in laser smoothing and micro-machining of optical glasses," Ph.D. dissertation (Heriot-Watt University, 2011).
3. Y. Hayasaki, T. Sugimoto, A. Takita, and N. Nishida, "Variable holographic femtosecond laser processing by use of a spatial light modulator," Appl. Phys. Lett. **87**, 031101 (2005).
4. Z. Kuang, W. Perrie, J. Leach, M. Sharp, S. P. Edwardson, M. Padgett, G. Dearden, and K. G. Watkins, "High throughput diffractive multi-beam femtosecond laser processing using a spatial light modulator," Appl. Surf. Sci. **255**, 2284–2289 (2008).
5. Z. Kuang, W. Perrie, D. Liu, S. P. Edwardson, J. Cheng, G. Dearden, and K. G. Watkins, "Diffractive multi-beam surface micro-processing using 10 ps laser pulses," Appl. Surf. Sci. **255**, 9040–9044 (2009).
6. D. Liu, Z. Kuang, W. Perrie, P. J. Scully, A. Baum, S. P. Edwardson, E. Fearon, G. Dearden, and K. G. Watkins, "High-speed uniform parallel 3D refractive index microstructuring of poly(methyl methacrylate) for volume phase gratings," Appl. Phys. B **101**, 817–823 (2011).
7. M. Silvennoinen, J. Kaakkunen, K. Paivasaari, and P. Vahimaa, "Parallel femtosecond laser ablation with individually controlled intensity," Opt. Express **22**, 2603–2608 (2014).
8. K. L. Wlodarczyk, J. J. J. Kaakkunen, P. Vahimaa, and D. P. Hand, "Efficient speckle-free laser marking using a spatial light modulator," Appl. Phys. A (2013), to be published.
9. Y. M. Xiao and M. Bass, "Thermal stress limitations to laser polishing of glasses," Appl. Opt. **22**, 2933–2936 (1983).
10. K. L. Wlodarczyk, I. J. Thomson, H. J. Baker, and D. R. Hall, "Generation of microstripe cylindrical and toroidal mirrors by localized laser evaporation of fused silica," Appl. Opt. **51**, 6352–6360 (2012).
11. M. D. Feit, M. J. Matthews, T. F. Soules, J. S. Stolken, R. M. Vignes, S. T. Yang, and J. D. Cooke, "Densification and residual stress induced by CO_2 laser-based mitigation of SiO_2 surfaces," Proc. SPIE **7842**, 78420O (2010).
12. E. Mendez Fernandez de Cordoba, "Laser micro-polishing of silica optics," Ph.D. dissertation (Heriot-Watt University, 2007).
13. C. Carey, W. J. Cantwell, G. Dearden, K. R. Edwards, S. P. Edwardson, J. D. Mullett, C. J. Williams, and K. G. Watkins, "Effects of laser interaction with graphite coatings," *Proceedings of the LANE* (2007), pp. 673–686.
14. K. L. Wlodarczyk, F. Albri, R. R. J. Maier, N. J. Weston, and D. P. Hand, "The impact of graphite coating and wavelength on picosecond laser machining of optical glasses," presented at the 31st International Congress on Applications of Lasers and Electro-Optics, Anaheim, California (2012), paper M309.
15. W. B. Pietenpol, "Surface tension of molten glass," J. Appl. Phys. **7**, 26–37 (1936).
16. W. D. Kingery, "Surface tension of some liquid oxides and their temperature coefficients," J. Am. Ceram. Soc. **42**, 6–10 (1959).
17. H. L. Schick, "A thermodynamic analysis of the high-temperature vaporization properties of silica," Chem. Rev. **60**, 331–362 (1960).
18. A. Q. Tool, "Relation between inelastic deformability of thermal expansion of glass in its annealing range," J. Am. Ceram. Soc. **29**, 240–253 (1946).
19. T. D. Bennett, D. J. Krajnovich, L. Li, and D. Wan, "Mechanism of topography formation during CO_2 laser texturing of silicate glasses," J. Appl. Phys. **84**, 2897–2905 (1998).
20. F. Wyrowski and O. Bryngdahl, "Iterative Fourier-transform algorithm applied to computer holography," J. Opt. Soc. Am. A **5**, 1058–1065 (1988).
21. J. S. Liu and M. R. Taghizadeh, "Iterative algorithm for the design of diffractive phase elements for laser beam shaping," Opt. Lett. **27**, 1463–1465 (2002).
22. J. S. Liu, M. Thomson, A. J. Waddie, and M. R. Taghizadeh, "Design of diffractive optical elements for high-power laser applications," Opt. Eng. **43**, 2541–2548 (2004).
23. R. Di Leonardo, F. Ianni, and G. Ruocco, "Computer generation of optimal holograms for optical trap arrays," Opt. Express **15**, 1913–1922 (2007).
24. S. Hasegawa and Y. Hayasaki, "Second-harmonic optimization of computer-generated hologram," Opt. Lett. **36**, 2943–2945 (2011).
25. R. J. Beck, J. P. Parry, W. N. MacPherson, A. Waddie, N. J. Weston, J. D. Shephard, and D. P. Hand, "Application of cooled spatial light modulator for high power nanosecond laser micromachining," Opt. Express **18**, 17059–17065 (2010).
26. J. P. Parry, R. J. Beck, J. D. Shephard, and D. P. Hand, "Application of a liquid crystal spatial light modulator to laser marking," Appl. Opt. **50**, 1779–1785 (2011).